Chapter

12

Acronyms Anonymous I: Spin Echo

12.1 Introduction

By now you will be familiar with the uses of the spin-echo (SE) sequence and its derivatives: TSE, STIR, FLAIR, 3D TSE, etc. In this chapter we delve a little deeper into the pulse sequence jungle, looking at the sequences from a more detailed and technical point of view, in particular how they are constructed to deliver the correct spatial and clinical information, and the limitations or compromises encountered in their use.

You will see that:

- segmented k-space acquisition schemes speed up SE-based acquisitions while retaining SE-like contrast;
- the effective echo time determines T_2 contrast in TSE;
- compromises are necessary: limited number of slices, increased spatial blurring and higher specific absorption rate (SAR);
- different types of RF pulses affect the image quality;
- single-shot turbo spin echo (TSE) and echo planar imaging (EPI) offer the ultimate speed for T_2-weighted imaging but with image quality compromises;
- radial TSE reduces movement artefacts.

To understand this chapter you need to be familiar with the material from Chapters 4, 8 and 9 and have some grasp of the concept of k-space. For each sequence examined we will answer the following questions: How fast is it? How does it localize signal? What contrast does it produce? How does it avoid artefacts? And are there any performance compromises required? An overview of the pulse sequence jungle was given in Chapter 4, now let's get in among the trees!

12.2 Conventional Spin Echo

Refer back to Chapters 3, 4 and 9 for details on echo formation, contrast appearance and clinical use of spin echo. The imaging gradients for a conventional SE sequence are shown in the right-hand side of Figure 12.1. These are similar to those illustrated in Chapter 8 for a GE sequence, but with a few differences: the 180° refocusing pulse and extra 'crusher' gradient lobes on its slice select (these prevent the 180° pulse from creating unwanted transverse magnetization), and the dephase lobe of the FE gradient now has the same sign as the readout portion. This is because the 180° pulse now forms the echo and spins must experience the same gradient moment before and after its formation to avoid phase errors.

We have seen that a clinical sequence also incorporates other features, e.g. fat saturation pulses and spatial saturation bands. These must be repeated within each TR period prior to the excitation of the imaging slice, and they take up time. These are shown in the left-hand side of Figure 12.1.

12.2.1 Limitations of Spin Echo

The basic reason for the slowness of conventional spin echo arises from the need to acquire each phase-encode line of the k-space raw data matrix from separate MR excitations, and the need to allow time for the magnetization to recover sufficiently between successive excitations. Addressing both of these problems, fundamental ways of speeding up an SE acquisition, other than the k-space tricks introduced in Chapters 6 and 8, are therefore:

- to acquire more than one line of data at once – this is called segmentation, used in fast or turbo spin echo (sometimes called RARE) – basically almost any sequence with the word 'fast' or 'turbo' in it;
- to 'cheat' the relaxation problem, by using restoration RF pulses;
- to use parallel imaging (Chapter 14).

Despite its slowness, spin echo has advantages that are worth keeping: its ability to generate T_1, T_2 and PD

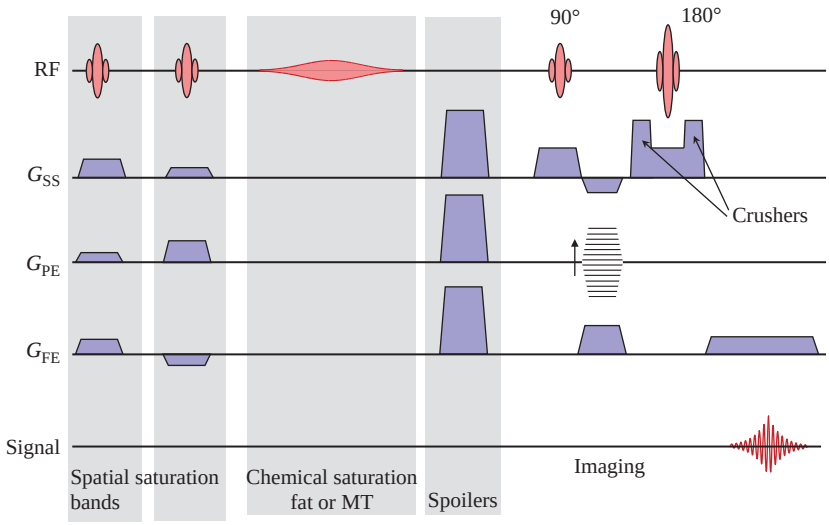

Figure 12.1 Imaging gradients for a simple SE sequence, including spatial saturation slabs and fat saturation pulses.

contrast, and its immunity from field inhomogeneity and susceptibility effects.

12.2.2 Multi-Echo Spin Echo

A precursor to the RARE segmented approach (TSE) is multiple spin echo, or 'multi-echo'. This is a conventional SE sequence but with multiple RF refocusing pulses applied to form a train of spin echoes (Figure 12.2). This process can be repeated for as long as sufficient transverse magnetization remains to form an echo, i.e. as long as T_2 relaxation permits. Each echo has the same phase encoding and thus a series of images of the same spatial location, but each with different T_2 weighting, is acquired. Since a long TR is required for good T_2 contrast, the additional TE images are acquired for 'free' in terms of scan time. For example, the use of a double echo acquisition with a short and a long TE enables one scan to produce a good anatomical (PD-weighted) image and a pathology (T_2-weighted) image. More details are given in Box 'Getting Focused on Spin Echo'.

Getting Focused on Spin Echo

In Section 9.4 we saw that multiple spin echoes were susceptible to accumulated RF flip angle errors and diffusion effects. For longer echo trains the Carr–Purcell–Meiboom–Gill sequence (CPMG) reduces these errors by changing the phase of the refocusing pulses with respect to the 90° pulse.

CPMG corrects every even echo for B_1 errors and produces echo amplitudes of the same algebraic sign. CPMG also reduces diffusion effects. An alternative scheme is a modified or phase-alternated Carr–Purcell (CP) scheme, where the RF phase angle is kept the same for both the 90° and the 180° pulses, but the algebraic sign of consecutive 180° pulses is alternated. This flips the transverse magnetization forwards (clockwise) and back (anti-clockwise) about the same axis and also assures that every second echo will lie properly in the *xy* plane in spite of B_1 errors. The sign of the echoes will alternate.

It is not entirely obvious that both CP and CPMG can also produce multiple unevenly spaced spin echoes. For example, in the dual echo sequence shown in Figure 12.2, the 'excitation' for the second echo is considered to occur at the time the first echo is formed. In this case

$$TE_1 = 2 \times T_A$$
$$TE_2 = 2 \times T_B; \text{provided } T_B \geq T_A$$

Note that phase encoding is only applied once after the 90° pulse and that the first frequency-encode gradient readout lobe acts as a dephase lobe for the second echo.

12.3 RARING to Go: Fast Spin-Echo Techniques

Images with SE-type contrast can be acquired with dramatic time saving by collecting more than one

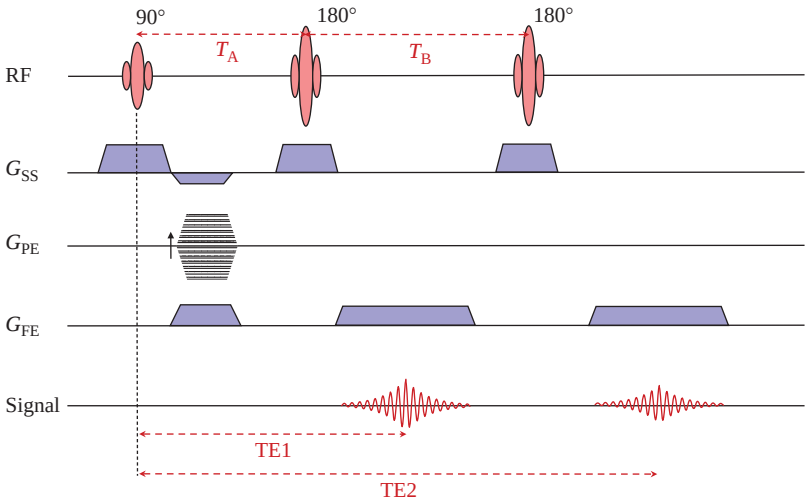

Figure 12.2 Dual echo imaging sequence. This produces two images with different TE but the same geometry.

line of data from a train of echoes formed by multiple refocusing RF pulses. This is known as segmentation. It can be achieved over several excitations and TR periods (multi-shots) or ultimately from a single shot. The T_2 contrast depends upon the ordering of the PE gradient steps or the filling pattern for k-space.

T_1 weighting can be achieved by using a short or intermediate TR as for conventional SE, or by using magnetization preparation, usually in the form of an inversion pulse. With TSE some resolution loss, in the form of blurring, may occur. Additionally, fat can appear very bright and some slice-to-slice variations in contrast may occur.

12.3.1 Turbo Spin Echo in Detail

Turbo **S**pin **E**cho (TSE), also known as **F**ast **S**pin **E**cho (FSE), is a commercial version of RARE (**R**apid **A**cquisition with **R**elaxation **E**nhancement) with evenly spaced multiple refocusing pulses (commonly, but not always, 180°) forming an echo train. These extra echoes are not used to acquire free images with different TE but are used to acquire multiple lines of data, i.e. different phase encoding applies for each echo (Figure 12.3). The **I**nter **E**cho **S**pacing (IES or ESP, **E**cho **SP**acing) is the time between successive echoes. This is always a fixed value as the RF pulses are all evenly spaced in time to avoid problems with coherence pathways (see Chapter 13). The echo train length (ETL) or turbo factor (TF) is the number of echoes in the spin-echo train.

The total scan time is

$$\text{Scan time} = \frac{\text{TR} \times N_{\text{PE}} \times \text{NSA}}{\text{ETL}}$$

A TSE sequence with, for example, 16 echoes (turbo factor of 16) will run 16 times faster than the equivalent spin echo. If TR is chosen to be 3 s, this means an acquisition requiring 12 min as a conventional spin echo will run in just 40 s. Sometimes TSE has an unusual number of phase-encode steps, as the latter has to be a multiple of the turbo factor. For example, if there are five echoes, the matrix could be 256 × 255 and a total of (255 ÷ 5) TR periods or excitations would be required.

In TSE, lines of k-space are acquired from different echoes and this affects the image contrast. The effective echo time (TE_{eff}) is the one that dominates the image contrast. We saw in Chapter 8 that the overall image brightness is primarily determined by the low spatial frequencies, those acquired with low step values of the phase-encode gradient. The centre of k-space dominates the image contrast. This is exploited in TSE, where TE_{eff} is arranged to coincide with the central segment of k-space (Figure 12.4). The order in which the phase encoding is applied affects the contrast, and various options are contained in Box 'Getting Wound Up: The Details of TSE'.

TSE can be PD-, T_1- or T_2-weighted in the same way as conventional spin echo. For T_1 weighting, where TR has to be relatively short, a smaller ETL may be required in order to achieve sufficient slice coverage. Dual-echo TSE is possible where the echoes

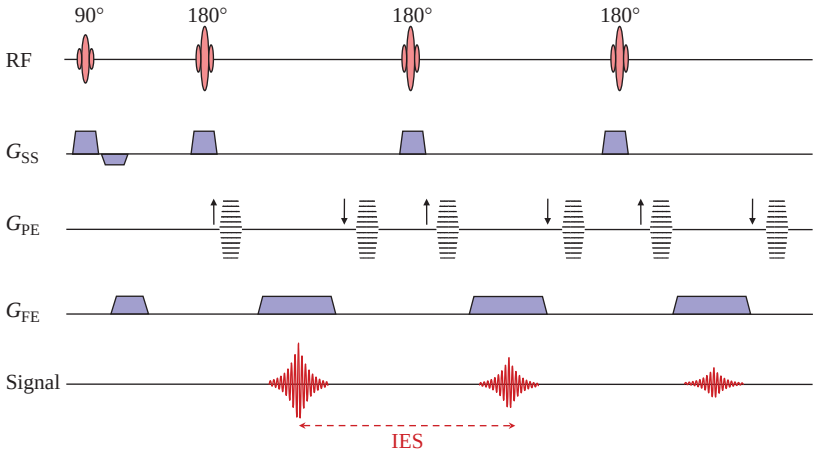

Figure 12.3 Turbo spin-echo sequence with an echo train length (turbo factor) of 3. IES denotes inter-echo spacing, i.e. the time between successive echoes.

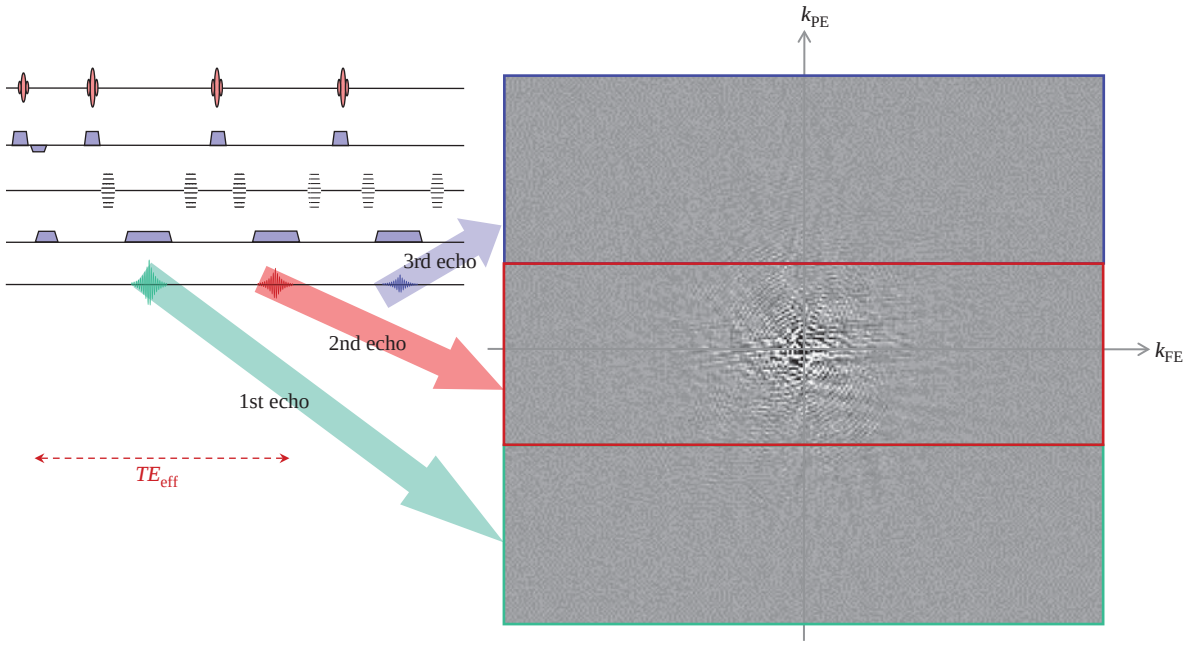

Figure 12.4 Data acquisition (k-space) filling for a three-echo TSE. The effective TE (TE_{eff}) is given by the time from the initial excitation to the second echo. Each point k_{FE} and k_{PE} represents a spatial frequency in the image

are divided between the different images with different TE_{eff}. This can be done by assigning the earlier echoes in the train to one image with a shorter TE and the later echoes to form a longer TE image. A more efficient way of achieving dual-echo TSE is by echo sharing, whereby some of the high spatial frequency data are shared between both images and only the low k-space data are encoded for more than one echo. Figure 12.5 shows spin-echo and TSE T_2-weighted images.

Getting Wound Up: The Details of TSE

In the sequence illustrated in Figure 12.3 the formation of the first spin echo is entirely conventional. In TSE the CPMG form of spin echo is used to avoid the accumulation of flip angle errors over the echo train (see Section 9.4). However, before we can acquire the second echo, we have to 'rewind' the phase encoding to undo the dephasing of the spins. To do this a phase-encoding step of equal strength but opposite

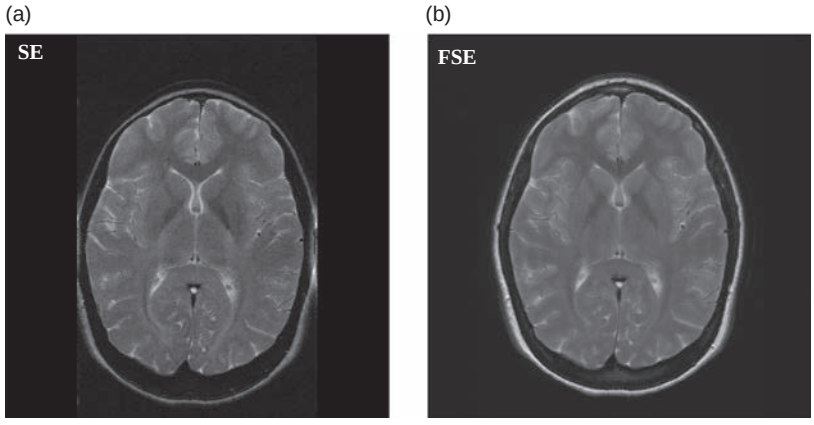

Figure 12.5 Representative images for spin echo (SE) and turbo spin echo (TSE) with similar TE. (**a**) SE: TR = 1500 ms, TE = 120 ms, scan time 4 min. (**b**) TSE: TR = 2735 ms, TE = 102 ms, ETL = 5, scan time 1 min 46 s. Note the appearance of fat, and the scan times.

in sign is applied after the completion of the data acquisition. In addition to rewinding, a form of phase correction of the data is required.

Each echo is responsible for a portion or segment of k-space. So different lines of k-space will have different T_2 weighting. The echo that contributes the central segment determines the effective echo time. By mixing the functions of contrast generation and localization, we have blurred the distinction between contrast and detail. Sequences with high values of ETL/turbo factor may display reduced spatial resolution. Additionally the echo train reduces the number of slices that can be acquired within the selected TR, approximately to

$$N_{\text{slices}} = \frac{\text{TR}}{\text{ETL} \times \text{IES}}$$

Also we can see from Figure 12.4 that we could assign any of the echoes to acquire the centre of k-space, thus changing the effective TE, sometimes known as asymmetric echoes, to achieve PD or T_1-weighting.

When a refocusing pulse of less than 180° is used, the signal will include contributions from stimulated echoes (see Box 'Echoes and coherences: Hahn and stimulated echoes' in Chapter 13), affecting contrast. For this reason, the rewinding scheme for phase encoding is applied in preference to 'blipping' (the accumulation of phase encoding from smaller, non-rewound phase-encoding steps) as used in EPI and GRASE (see Section 12.5).

12.3.2 A Compromising Situation

So is TSE 'the best thing since sliced bread'? Not quite; there are compromises involved, including reduced slice numbers, higher RF exposure, complicated contrast behaviour and possibly reduced resolution.

The slice number restrictions will be apparent to anyone who has sat at the MR console planning a TSE scan. We saw in Section 8.4.3 how slice interleaving within the TR is used to deliver multiple slices within the same overall acquisition time. As the time occupied by the longer echo train in TSE is greater, it reduces the possibility of acquiring a large number of interleaved slices within the TR. To compensate for this, a longer TR can be used with an increased scan time for T_2- or PD-weighted images, but not for T_1-weighted images.

However, even if the required number of slices can be reconciled with the ETL and TR required, you often find your plans thwarted by the scanner on account of SAR limits. The SAR (explained further in Section 20.2) is a measure of the patient's RF exposure and is subject to national and international limits. TSE techniques with their many large RF pulses can very easily exceed the SAR limit, particularly at higher field strengths. To reduce the SAR to an acceptable level you need to reduce the number of slices, increase the TR, reduce the ETL or reduce the flip angle of the refocusing pulses (see Box 'Turning Down the Heat: Reducing SAR'). This latter is possible on some scanners and usually solves the SAR limitation problem, but at the cost of some reduction in SNR. In a properly constructed sequence it does not cause artefacts.

We Still Use Conventional T_1-Weighted SE. Why?

T_1w imaging, particularly of the brain and spine, requires TR in the range 400–600 ms for a 1.5 T scanner. If we are acquiring 3 mm slices we will need more than 30 to fully cover the cerebrum,

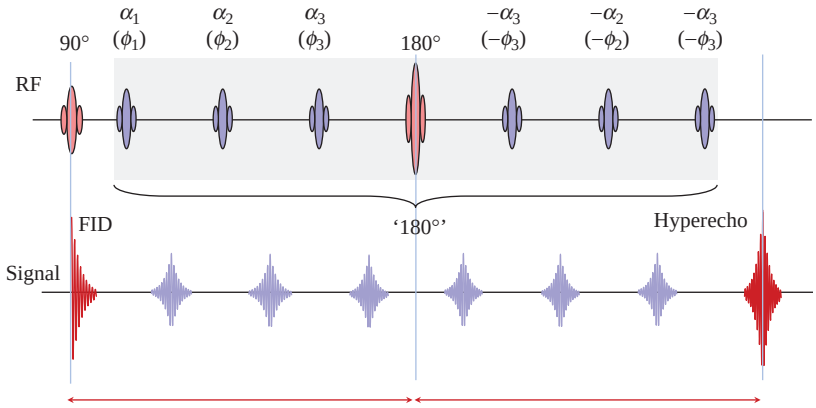

Figure 12.6 TSE echo train showing reduced refocusing angles and the hyperecho formed by making the fourth refocusing pulse a full 180° pulse.

giving us less than 20 ms per slice. If we further divide k-space into three (the minimum) segments, we have less than 7 ms to acquire each echo. This is not long enough. It is simply better to use 'old-fashioned' SE for this acquisition. It has further advantages of lower SAR and less T_2 blurring, insensitivity to flow artefact and responds in a predictable manner to Gd contrast.

Turning Down the Heat: Reducing SAR

The TSE pulse sequence has a high SAR per unit time, particularly on high-field scanners since the SAR is proportional to B_0^2. One way of reducing this effect is to use smaller flip angles during the refocusing echo train. You would think that the expected signal amplitude would be reduced with this scheme. However, a number of extra coherence pathways (see Box 'Coherence Pathways' in Chapter 13) are formed, including stimulated echoes, and these can combine to produce spin echoes with larger signals. Of course, the contribution from stimulated echoes means that the contrast is a function of both T_2 and T_1.

It can be shown that the signal forms a 'pseudo-steady-state' (ignoring relaxation effects) proportional to $\sin(\theta/2)$. Furthermore, the signal can be 'catalysed' into the steady state by choosing the first few refocusing pulses to have specific flip angles. For example, if the first refocusing pulse is a $(90 + \theta/2)°$ pulse, and θ is the flip angle of the rest of the refocusing train, the echo amplitude is close to the maximum theoretical amplitude.

The reduced SNR can be further recovered by using 'hyperechoes'. A hyperecho is produced by using a 180° refocusing pulse in a train of reduced θ refocusing pulses. By arranging the timing so that the hyperecho occurs when the centre of k-space is acquired, the overall image SNR will be increased. Figure 12.6 shows a train of seven refocusing pulses, with the fourth pulse a full 180° and the others reduced. The hyperecho occurs after the seventh refocusing pulse, and has an amplitude almost equal to that achieved by a conventional train of 180° pulses.

If the low values of phase encoding in the centre of k-space determine the overall image contrast, what do the higher k-space data contribute? They determine the high-frequency or detailed content of the image and their relative strength may be emphasized or reduced, depending on the k-space ordering scheme employed. If the high frequencies are acquired for longer actual TE then they will be attenuated by T_2 relaxation and some spatial resolution will be lost. If they are acquired at a shorter TE than the effective TE they will be emphasized, which may lead to excessive ringing or Gibbs' artefact. For this reason additional filtering may be applied for TSE sequences.

A major consequence is that the spatial resolution will depend on the T_2 of the tissues. In practice, an arbitrarily large echo train length cannot be used without impairing the spatial resolution (Figure 12.7). This is most apparent in single-shot techniques such as HASTE (see Section 12.4.3). However, while it is true that sequences with large turbo factors may lead to blurring or resolution loss compared with a non-segmented sequence such as spin echo, TSE offers the opportunity to acquire large matrices (512 × 512 or even 1024 × 1024) and therefore produce very high-resolution images within a reasonable scan time.

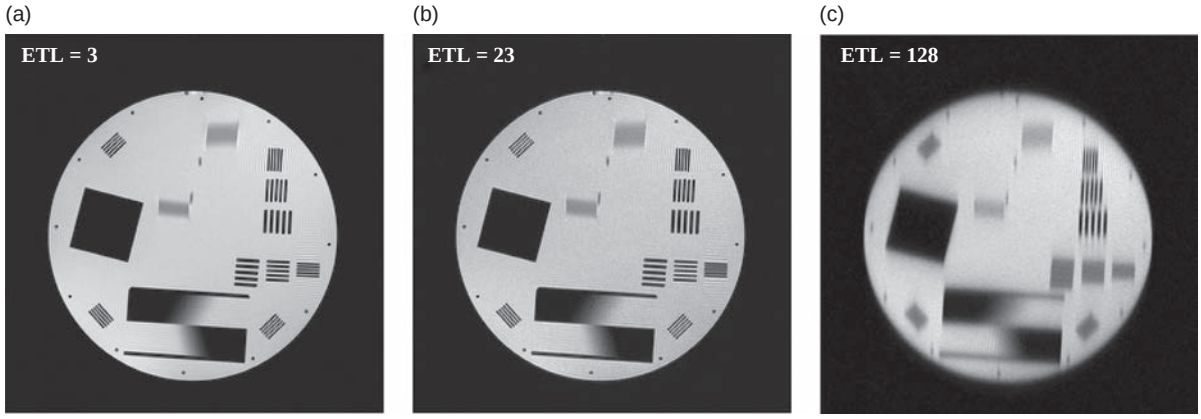

Figure 12.7 Resolution in segmented sequences showing resolution loss in the phase-encode (PE) direction. (a) TSE with three echoes (ETL = 3), TR = 600 ms, TE = 12 ms, scan time 52 s. (b) TSE with 23 echoes, TR = 600 ms, TE = 128 ms, scan time = 6 s. (c) HASTE (ETL = 128), single shot ('TR' = ∞), TE = 87 ms, scan time = 1 s. Phase encode is vertical. Note the subtle resolution loss for ETL = 23, and the major resolution loss for HASTE. The phantom fluid had a T_2 of 200 ms.

A final issue of compromise relates to the appearance of fat in the images. In TSE fat is bright, as shown in Figure 12.5. Bright fat may be useful, particularly in the abdomen where it outlines all of the organs and bowel. However, it may also reduce the dynamic range available in the image and therefore obscure subtle contrast changes (e.g. in the knee), or sometimes it may result in a high level of motion artefact (e.g. from the highly mobile suborbital fat) or conceal pathology. This can be addressed by applying further pre-pulses in the form of fat suppression by a number of techniques (see Chapter 7). Further details are given in Box 'Is TSE the Same as SE?'.

Is TSE the Same as SE?

The image contrast in TSE is not the same as for SE. The multiple RF pulses result in the generation of stimulated echoes in TSE which add to the spin-echo component of the signal.

In particular, fat appears very bright in TSE. Actually, it is conventional spin echo that depicts fat less bright than expected for a tissue with its combination of short T_1 and relatively long T_2. The reason lies with *J*-coupling, which is an interaction between different nuclei within the fat molecule and results in a shortening of T_2. In TSE the rapid train of refocusing pulses breaks this coupling and thus fat signals have effectively a longer T_2 and appear brighter in the image.

A TSE sequence designed to conserve the *J*-coupling effect and look more like spin echo is DIET (**D**elayed **I**nterval **E**cho **T**rain), which has a longer IES for the first pair of refocusing pulses. At the time of writing this is only commercially available on Toshiba systems.

The application of various fat suppression techniques is common for TSE imaging. Additionally, there may be slice-to-slice variations in image contrast. This may be due to unwanted magnetization transfer interactions caused by off-resonance RF from adjacent slices.

In GRASE imaging (Section 12.5) the use of intermediate gradient echoes between each spin echo means that a longer IES (for the 180° pulses) can be employed. This may conserve the *J*-coupling and produce images that are more spin-echo-like.

12.4 The Extended Family of TSE

12.4.1 Inversion Recovery TSE

The use of turbo spin echo to obtain T_1 weighting with shorter TR is limited by compromises between the number of slices achievable and the echo train length (ETL). It is possible, however, to achieve T_1 weighting by the addition of a preparation pre-pulse in the form of an inversion combined with a high ETL, i.e. as inversion recovery TSE (or IR-TSE or turbo-IR). One of the downsides of conventional inversion recovery is the long scan time involved because of the need for a TR of at least three (and preferably five) times the T_1 of tissue. Combining IR

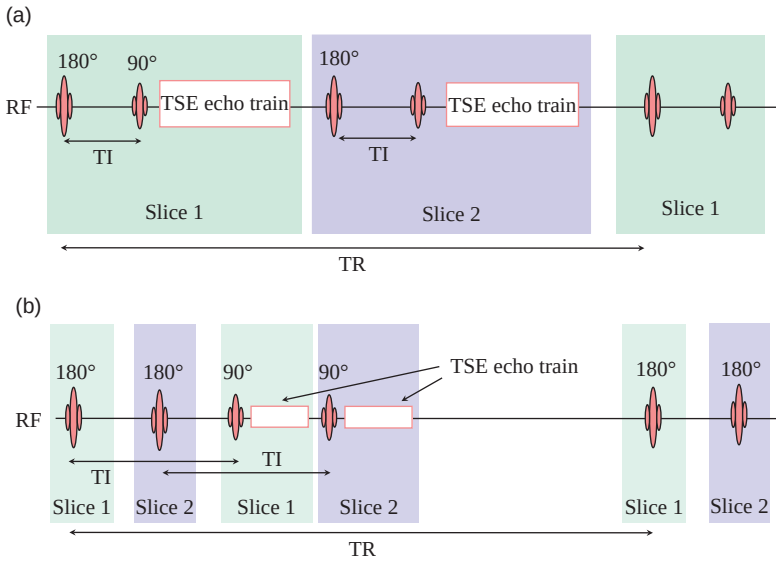

Figure 12.8 Interleaving schemes for inversion recovery TSE: (a) sequential where each TI is completed before incrementing the slice; (b) interleaved where more than one slice is inverted within each TI.

with TSE enables the use of the long TR required but with a clinically acceptable scan time. The T_1 contrast is conventional and is primarily determined by the inversion time (TI).

Clinical applications of this include Short TI Inversion Recovery (STIR), in which a short TI is used to null the fat signal and something akin to T_2-weighted appearance is achieved in the image (Section 3.7), and FLAIR imaging (Section 3.4) where a long TI (e.g. 2000 ms) combined with a long TR (up to 10 s) is used to null the cerebrospinal fluid (CSF) signal in neuro-imaging. The use of k-space segmentation makes the scan time for FLAIR clinically acceptable. Another application is real-reconstruction (or true) inversion recovery, useful for examining the degree of myelination in the immature brain, where the inversion pulse is used to improve contrast.

The combination of IR with TSE involves certain complications over how slice interleaving is achieved. There are compromises regarding turbo factors (ETLs), TI and TR, which are examined in Box 'Interleaved IR-TSE'. The scan time is given by the same expression as for TSE; however, there may be limitations on the number of slices achievable. With IR-based techniques there are also limitations in the spatial quality of the inversion pulses (see Box 'More on RF Pulses'). It is common in IR-TSE to have a significant gap between slices and to use an interleaved slice order to avoid crosstalk.

An improvement in the quality of the inversion can be achieved by using adiabatic pulses (see Box 'Adiabatic RF Pulses'). This is particularly important when the uniformity of the B_1 transmission field is poor, as may occur at 3 T. Adiabatic inversion methods are known as **S**pectrally **A**diabatic **I**nversion **R**ecovery (SPAIR) by Siemens; **SP**ectral **A**ttenuated **I**nversion **R**ecovery (SPAIR) by Philips; or **A**diabatic **S**pectral **I**nversion **R**ecovery (ASPIR) by GE Healthcare.

Interleaved IR-TSE

The potential for slice interleaving in TSE sequences is reduced because the data-acquisition time is longer to encompass the whole echo train. This presents special problems for inversion recovery, where each slice has to undergo inversion at a time TI before the signal readout/spatial encoding part of the sequence. We have two options for arranging the slices shown in Figure 12.8:

(a) Interleave within the TR, i.e. invert and readout one slice before inverting the next one. In this case the maximum number of slices is

$$N_{slices} = \frac{\text{TR}}{\text{TI} + (\text{IES} \times \text{ETL})}$$

For very long TI such as those used in FLAIR this restricts the number of slices obtainable for a given TR and the number is dependent upon the TI you chose. It works best for short TI, such as in STIR. This scheme is sometimes referred to as 'sequential'.

(b) Interleave within TI, i.e. we invert all the slices first within the time TI and then read them all out. The

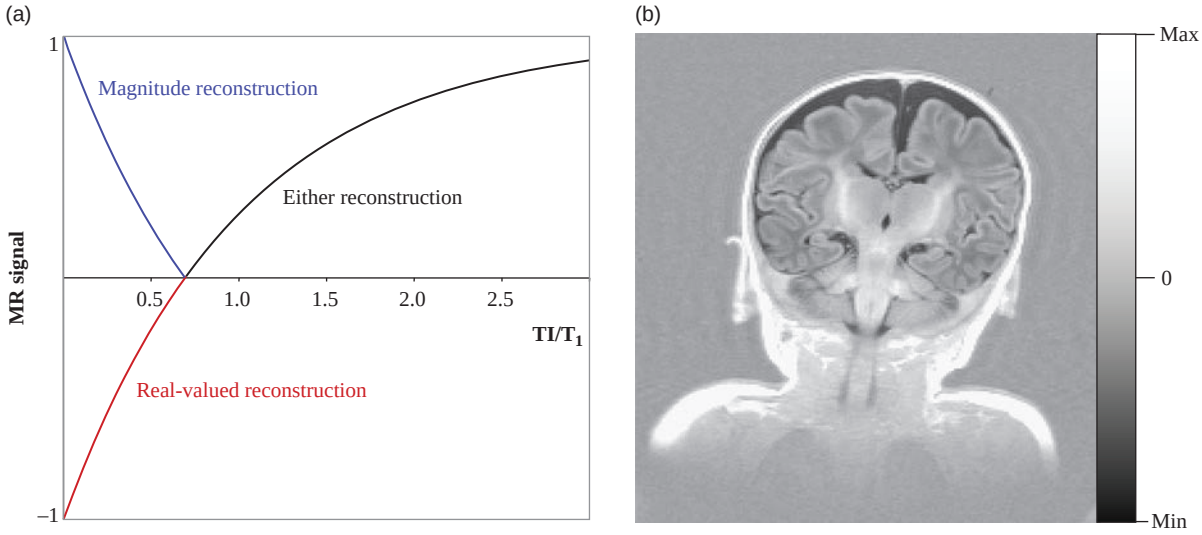

Figure 12.9 (a) Signal dependence of real-valued IR. (b) Example of true inversion recovery sequence of an infant brain. The image background is mid-grey, allowing the display of both positive and negative MR signals

number of slices is now independent of TR but depends upon TI:

$$N_{\text{slices}} = \frac{\text{TI}}{(\text{IES} \times \text{ETL})}$$

Obviously for very high turbo factors, the number of slices is going to be restricted. A compromise between number of slices and speed of acquisition is usually required. This arrangement works best for long TI, e.g. for FLAIR, and is sometimes called 'interleaved'.

Inversion recovery offers the possibility of the MR signal being positive or negative. Usually MR images are presented in magnitude form, i.e. with no negative values, the sign of the signal being ignored in the final image (this is to overcome artefact problems arising from phase changes due to susceptibility variations and magnet inhomogeneity). With real-valued inversion recovery, the image is reconstructed in real rather than magnitude mode, i.e. with positive and negative voxel values (Figure 12.9a). This means that the background is mid-grey and the image values range from black to white. Exceptionally good contrast, particularly in brain tissues, is achievable with true inversion recovery. Figure 12.9b gives an example for a neonatal brain.

More on RF Pulses

Selective pulses, as seen in Section 8.4, utilize a shaped RF pulse in conjunction with a gradient. If the pulse generates transverse magnetization, i.e. if it is anything but a refocusing pulse, it is usually necessary to have a rephase gradient to ensure that the transverse magnetization points in the same direction. The rephase portion has half the gradient moment of the selective part and the opposite sign. For a 180° pulse, rephasing is not required. In the case of a refocusing pulse (i.e. in spin echo), the gradient is self-rephasing. For an inversion pulse, there is no transverse magnetization (ideally) and the selective gradient ideally produces no phase changes.

Selective slices are not uniform in the selection direction, but have a variation in flip angle perpendicular to the image plane they define, known as the slice profile. A consequence is that for a 180° pulse there will be regions where magnetization is partially tipped into the transverse plane (at some point the flip angle will pass through 90°).

For a refocusing pulse a pair of 'crusher' gradients, as shown in Figure 12.10, can overcome this problem. These are equal gradients applied either side of the refocusing pulse. Refocused magnetization that goes on to form an echo will have seen both gradients and, because of refocusing, will be unaffected. However, fresh free induction decay (FID) created by the refocusing pulse only experiences one gradient lobe and will be dephased.

In practice it is quite difficult to achieve good inversion, e.g. in inversion recovery sequences. Particularly at higher field strength, 'adiabatic' pulses

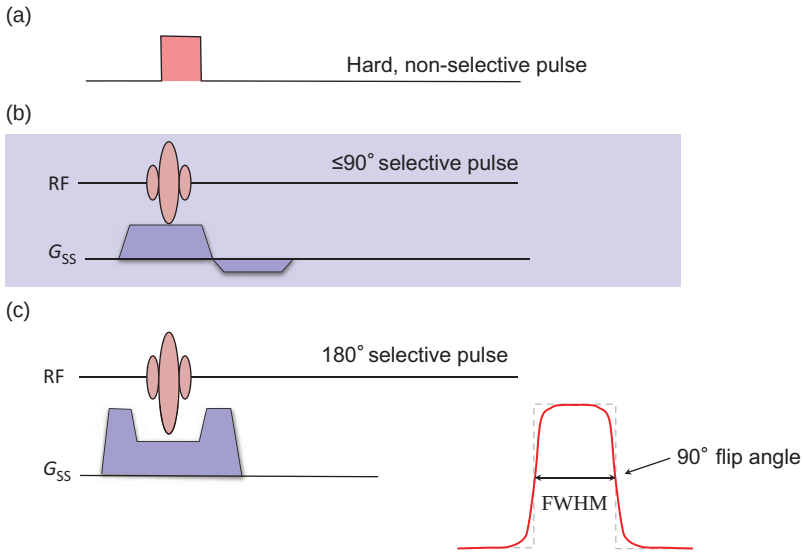

Figure 12.10 Types of RF pulse. (a) Hard, non-selective pulse. The RF is applied as a short, broad bandwidth pulse. (b) Selective excitation pulse. The spectrally shaped RF pulse is applied simultaneously with a slice-select gradient. A rephase gradient lobe is required to correct phase shifts. (c) Selective 180° pulse. No rephasing is necessary, but crusher gradient lobes are required. The slice profile shows that at some point along the selection axis the flip angle will be 90°.

provide more uniform inversion (see Box 'Adiabatic RF Pulses') since they are less sensitive to B_1 inhomogeneities. For single-shot sequences with an inversion pre-pulse, the inversion pulse may be non-selective. A non-selective pulse is applied without a gradient, so it has no spatial localization. Subject to the RF coil's homogeneity and tissue RF absorption, it will have the same effect at all points of space. A non-selective pulse can have any temporal waveform, and it is advantageous to keep the pulse short, a rectangular waveform being common. Such pulses are often called hard pulses.

Composite RF pulses, or 'binomial' pulses, are often used for spectral excitation, i.e. to obtain a signal from either water or fat. These pulses are made up of a series of either selective or hard pulses and are always followed by spoiler gradients to 'mop up' any residual fat signal (see Box 'Water-Only Excitation').

Adiabatic RF Pulses

Adiabatic pulses behave quite differently to normal RF pulses. They use both amplitude and frequency modulation to pull the magnetization away from the z axis. If this sounds weird, it's because adiabatic pulses are weird! To explain them, we have to go back to the rotating frame and consider how the protons precess around an RF magnetic field.

Previously we have assumed that B_1 is applied at the Larmor frequency along x' or y' in the rotating frame. However, if the frequency of the RF is slightly off resonance there is also a component of B_1 in the z' direction. In this situation, the transverse and longitudinal components of B_1 combine to give an effective field B_{eff} at an angle ψ to the z' axis. When the amplitude of B_1 is small or the RF frequency is a long way off resonance, B_{eff} is very close to the z' axis; as the amplitude is increased and the frequency is exactly on resonance, B_{eff} is exactly in the transverse plane.

The magnetization obeys the Larmor equation and precesses (in the rotating frame) about B_{eff} (Figure 12.11a). If we create an RF pulse such that B_{eff} is initially in the z' direction, then gradually change the amplitude and frequency so that B_{eff} slowly rotates towards the transverse plane, the magnetization will continue to precess about B_{eff} until it is also precessing in the transverse plane. If the pulse is now switched off, lo and behold, the magnetization is in the transverse plane and can give us an MR signal. The only constraint is that the changing angle of B_{eff} is much less than the precessional frequency about B_{eff}, described mathematically by

$$\frac{d\psi}{dt} \ll \gamma B_{\text{eff}}$$

This can be achieved by choosing a strong effective field (high B_1) or a slow frequency modulation. The term 'adiabatic' comes from Greek, meaning 'impassable to heat', and is used in thermodynamics to describe processes where no external energy is used. Returning to the idea that protons absorb energy from a normal RF pulse during excitation, we can think of adiabatic pulses as forcing the protons to use their own internal energy to change

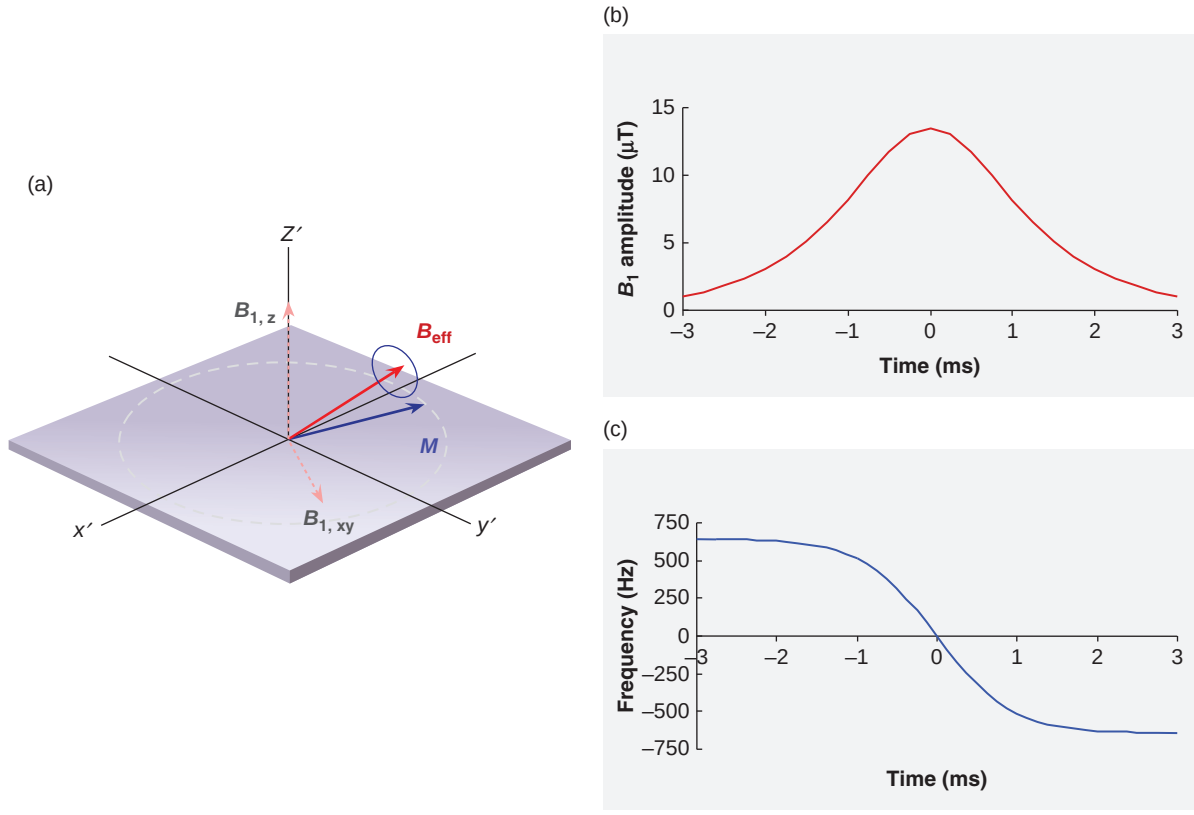

Figure 12.11 Adiabatic pulses. (a) When the RF is slightly off resonance, B_{eff} is at an angle between z' and the transverse plane and protons precess about B_{eff}. (b) Amplitude and (c) frequency modulation for a hyperbolic secant (sech) adiabatic inversion pulse. Note that the amplitude starts low, increases to a maximum and then returns to zero, and that the frequency is swept from several hundred hertz below ω_0 to several hundred hertz above.

their orientation. No energy is absorbed from the RF pulse, so the spin temperature does not change. We warned you that these are weird pulses!

Different types of amplitude and frequency modulation can be used to create adiabatic pulses for excitation, inversion or refocusing. For example, the hyperbolic secant pulse is popular for inversion; Figure 12.11b,c shows the amplitude and frequency modulation of the pulse. All adiabatic pulses have the major advantage of being insensitive to B_1 inhomogeneities, making them particularly useful at higher field strengths.

Water-Only Excitation

Instead of saturating the signal from fat, an alternative approach is to excite only the water signal. Binomial pulses are one such way to achieve water-only excitation. Binomial pulses consist of a series of RF pulses with flip angles following a binomial series such as 1:1. The interval between the pulses τ equals the time for fat and water to become 180° out of phase, i.e., $\tau = 2.3$ ms at 1.5 T. The simplest example is a 1-τ-1 pulse shown in Figure 12.12. First a 45° pulse is applied along the $+x'$ axis, then the fat and water protons are allowed to dephase. When they are exactly out of phase, a second 45° pulse is applied, taking the water protons into the transverse plane and returning the fat protons to the longitudinal direction. Other binomial pulse schemes use a 1:2:1, and 1:3:3:1 sequence, i.e. 22.5°-τ-45°-τ-22.5° or 11.25°-τ-33.75°-τ-33.75°-τ-11.25°. The use of a 1:1 pulse essentially provides a sinusoidal modulation with a very narrow-band saturation of fat, whereas increasing the number of pulses results in a broader fat suppression (Figure 12.12) at the cost of an increase in duration of the excitation.

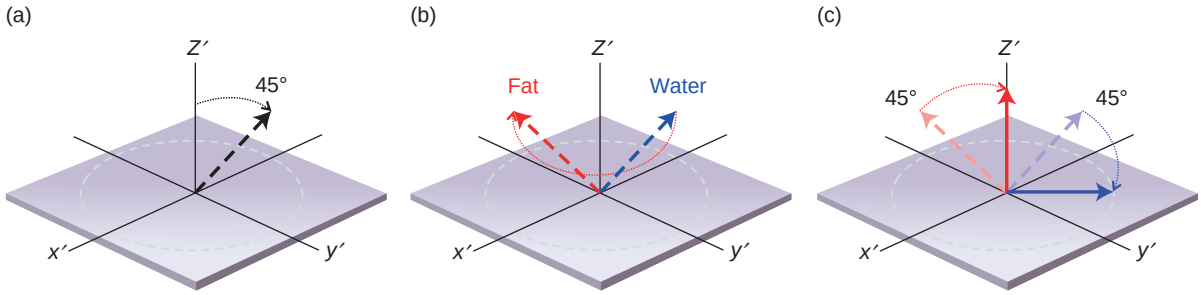

Figure 12.12 A 1:1 binomial pulse suppresses fat by (a) exciting both water and fat, (b) allowing time for the fat to dephase by 180°, then (c) applying a second 45° pulse to leave the water protons in the transverse plane and the fat protons returned to the *z* axis.

Binomial pulses are more robust against B_0 homogeneity; however, they are usually achieved with hard (rectangular) pulses which means they are most suitable for 3D imaging, not multi-slice 2D. If the hard pulses are replaced by slice-selective pulses, then they become B_0-sensitive. If the binomial pulses are slice selective then the pulse train is known as a spectral-spatial excitation. Different manufacturers will have slightly different implementations of spectral-spatial pulses. The Philips binomial implementation, for example, is called PROSET (**PR**inciple **O**f **S**elective **E**xcitation **T**echnique).

12.4.2 Drive Time: Driven Equilibrium

Driven **E**quilibrium (DE) is a technique to drive the magnetization back to the positive *z* axis (towards equilibrium) by using an additional RF pulse rather than through longitudinal relaxation, which is a much slower process. Transverse magnetization can be driven back towards equilibrium by a 90° pulse on the $-x'$ axis (–90°), as in Figure 12.13a. This enables a shorter TR to be used in TSE sequences. DE works best for tissues with longer T_1 and T_2, where the residual magnetization lies mainly in the transverse plane and has a relatively low amount of dephasing. It is therefore good for imaging fluids.

12.4.3 Single-Shot TSE and HASTE

The ultimate turbo sequence is single-shot TSE, where there is only one initial RF excitation (90°) pulse followed by a very long echo train over which all the phase-encode steps are acquired. This type of sequence is applied sequentially for multiple slice acquisitions, i.e. a whole slice is acquired at a time before moving on to the next slice. Usually an inter-slice delay (time delay or TD) is required between successive slices. The scan time will therefore be

$$\text{Scan time} = N_{\text{slices}} \times (\text{scan time for slice} + \text{TD})$$

With this type of sequence there will necessarily be significant T_2 signal decay over the course of the acquisition and hence its clinical use is limited to the study of predominantly fluid structures, such as the biliary system, as a technique for MRCP (see Box 'MR Cholangiopancreatography') and Figure 12.14.

HASTE (Half Fourier Single Shot TSE) is a form of single-shot TSE available on Siemens scanners, which uses a phase-alternated CP echo train combined with half Fourier acquisition (Section 8.7.1). HASTE produces a moderate spatial resolution (256 × 128 or 240) with a moderate to long TE (60–120 ms) giving T_2-weighted images. It can also be combined with an inversion recovery pre-pulse to give a single-shot variant of STIR or FLAIR. Often non-selective inversion pulses will be used (see Box 'More on RF Pulses'). In this case a sufficient inter-slice delay is required to ensure full recovery to equilibrium of the inverted magnetization.

So why don't we use single-shot sequences all the time? The answer lies in the compromises involved with all segmented spin-echo techniques, of which single-shot-TSE and HASTE are the most extreme examples, and therefore the most extremely compromised. The single-shot image in Figure 12.14a (HASTE) clearly results in impaired spatial resolution. However, this limitation must be weighed up against the benefit of taking only 1 s to acquire, which effectively eliminates bowel and respiratory motion.

MR Cholangiopancreatography

The MRCP is a common examination which investigates the biliary and ductal system of the liver and

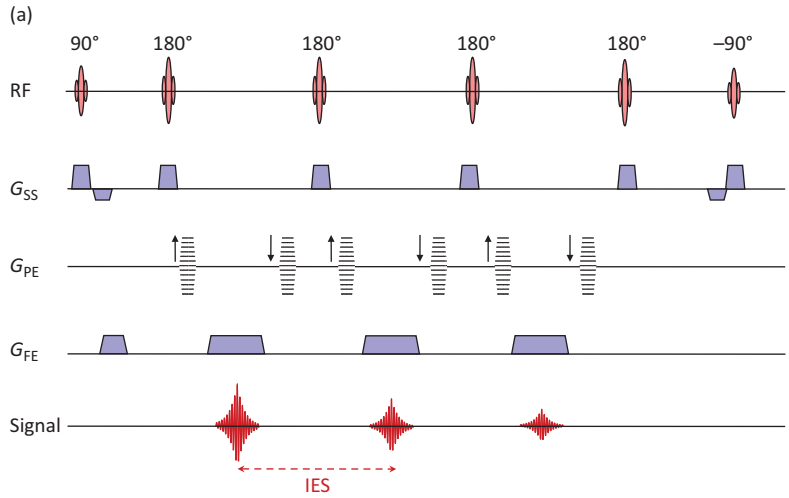

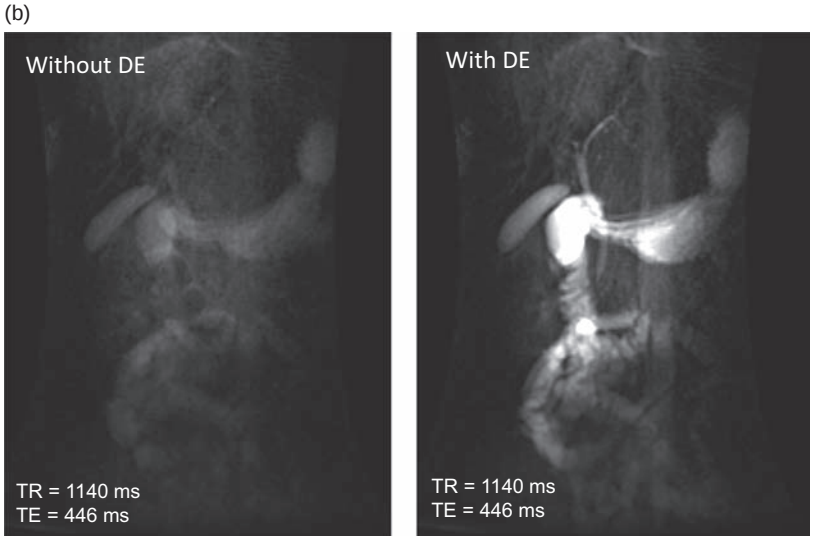

Figure 12.13 (a) Pulse sequence diagram for TSE with driven equilibrium. (b) TSE MRCP images without (left) and with (right) driven equilibrium. TR = 1146 ms, TE = 446 ms.

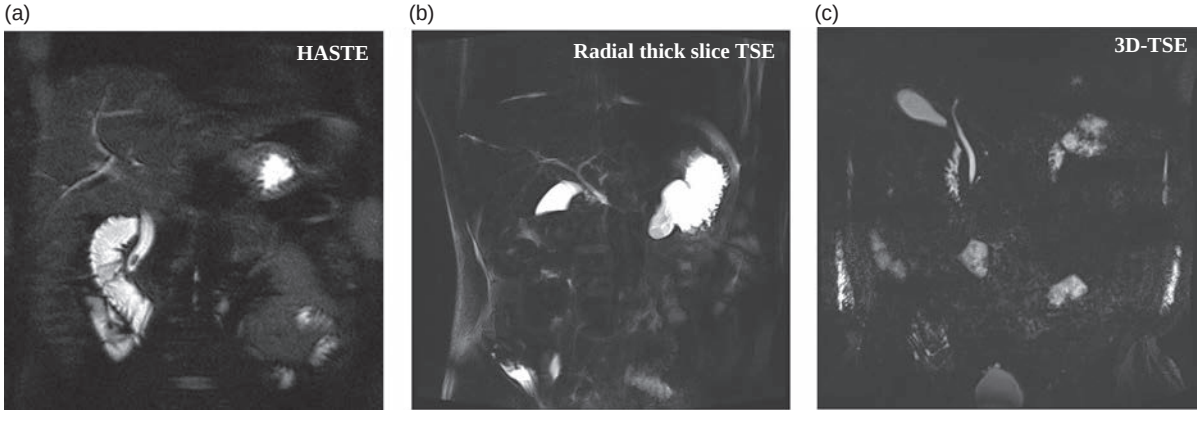

Figure 12.14 Half Fourier single-shot TSE (HASTE) and single-shot TSE images (MRCP). (a) HASTE, slice thickness 5 mm. (b) Radial SS-TSE, thick slab (50 mm). (c) 3D TSE, 1 mm slice.

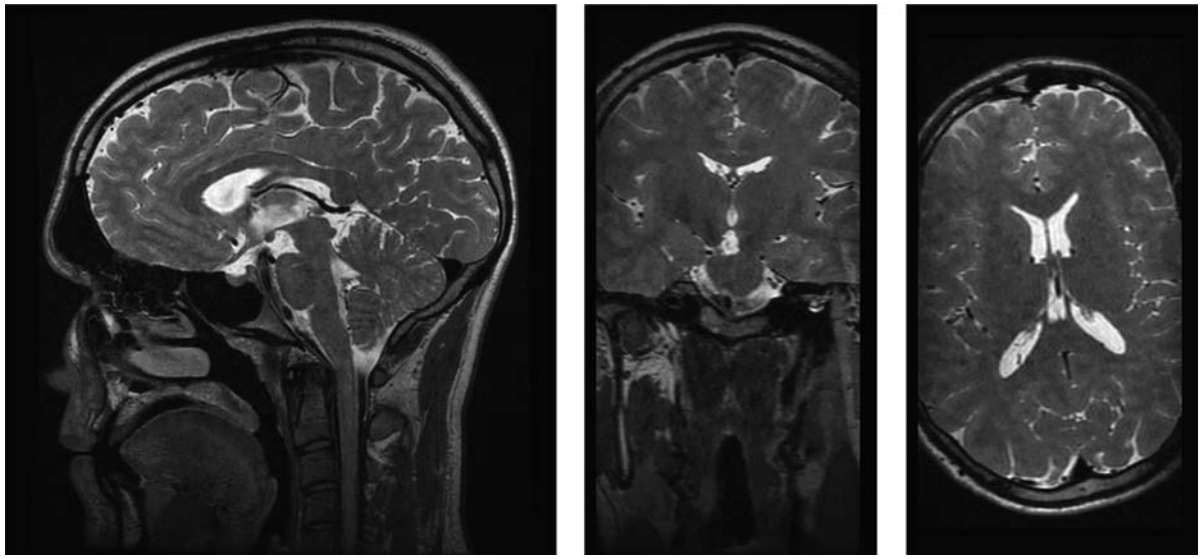

Figure 12.15 3D TSE SPACE images and reformats of the brain.

pancreas. The ducts and gall bladder can be visualized using a very long TE – of at least 500 ms. This ensures that all other signals have decayed, leaving just the bile fluid. Single shot TSE methods are ideal for this as they enable entire slices to be acquired in a breath-hold. Three imaging strategies are common:

1 Multi-slice SS-TSE or HASTE, with slice width 5–10 mm (Figure 12.14a).
2 Radially arranged SS-TSE/HASTE thick slices of typically 50 mm, which resemble MIPs without the post-processing. Only a small number of angled coronal slices are required (Figure 12.14b).
3 A third strategy is to acquire a 3D RF-modified TSE (SPACE, CUBE, 3DVIEW, etc.). This can supply the same information, but with high resolution, e.g. 1 mm isotropic, from which MIPs and MPRs can be calculated (Figure 12.14c).

12.4.4 3D TSE

As we saw in Section 8.8, by adding an extra phase-encode gradient series, acquisitions can be made three-dimensionally. 3D FT offers the prospect of very thin 'slices' or even isotropic voxels which makes the acquisitions suitable for multi-planar reformatting. Conventional spin echo is not practical as a clinical 3D sequence because of its long scan time. However 3D TSE offers scan times of just a few minutes. The scan time is

$$\text{Scan time} = \frac{\text{NSA} \times N_{\text{PE1}} \times N_{\text{PE2}} \times \text{TR}}{\text{ETL}}$$

and is kept short by using a high ETL or turbo factor and possibly partial Fourier and parallel imaging. The sequence gives the geometric and SNR advantages inherent in a 3D acquisition, while retaining the TSE features of long TE (T_2 weighting) and long TR.

In order to avoid artefacts and to keep within SAR limits, some tricks have to be done with the RF pulses (see Box '3D-views by Spacey Cubists: 3D TSE'). Figure 12.15 shows an MPR from an RF-modified 3D TSE image. These sequences produce T_1, T_2, PD and FLAIR contrast and are good for inner ear, joints and MRCP examinations. Vendor acronyms are given in Table 4.1.

3D-Views by Spacey Cubists: 3D TSE

With a conventional train of spin echoes, the echo height decays with the time from the initial excitation, so for the *n*th echo in TSE

$$E(n) \propto M_0 \exp\left(-\frac{n \cdot \text{IES}}{T_2}\right)$$

where IES is the inter-echo spacing. For very long ETL of the order of 100–200, the signal decay from most tissues will be unacceptably large.

In 3D TSE (SPACE, CUBE, 3DVIEW, etc.) the IES is minimized by using non-selective refocusing pulses.

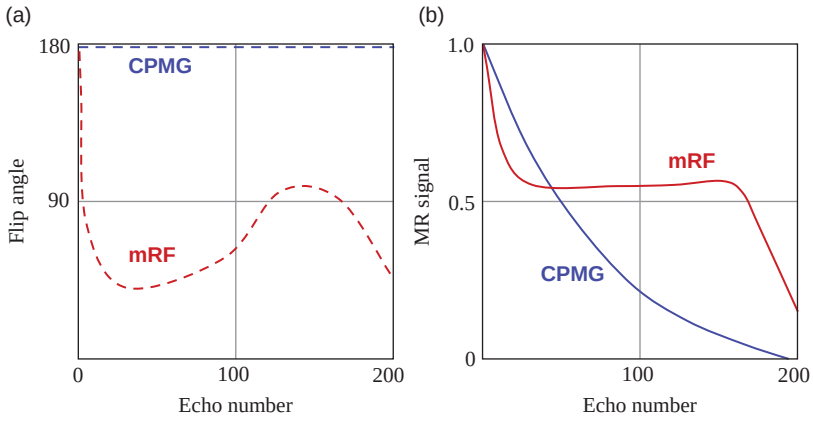

Figure 12.16 Example of RF flip angle and signal evolution for conventional TSE (CPMG) shown in blue and RF-modified 3D TSE shown in red.

Additionally, the flip angle is modulated throughout the echo train, starting large and decreasing to a smaller value of typically 30–60°. The use of smaller flip angles results in some of the transverse magnetization being temporarily 'stored' as longitudinal magnetization. As T_1 is generally longer than T_2, this means that the signal intensity from the echo train is maintained for longer than in a conventional CPMG echo train. In 3D TSE the echoes are formed as a combination of spin echoes and stimulated echoes (see Box 'Echoes and coherences: Hahn and stimulated echoes', in Chapter 13). Figure 12.16 shows a schematic of the RF pulse modulation and echo height for a conventional CPMG and a 3D TSE acquisition. The use of lower flip angle refocusing pulses also minimizes SAR.

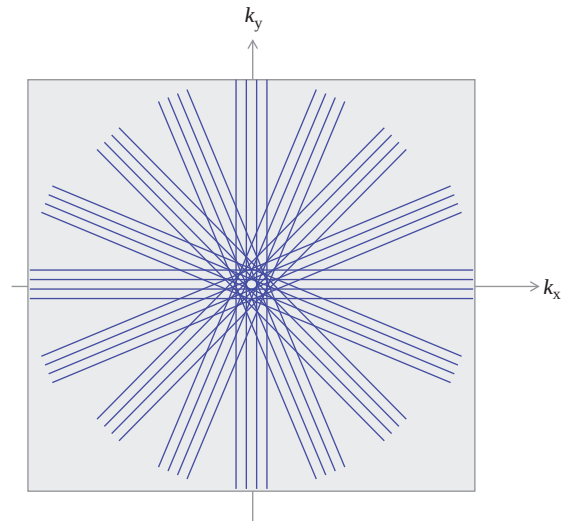

Figure 12.17 k-space trajectories for radial TSE acquisition (PROPELLER) with four echoes per blade and eight blades.

12.4.5 Radially Acquired TSE

One of the downsides of TSE is its sensitivity to motion artefact. Radial k-space acquisition is a way to overcome this problem. Originally called PROPELLER (**P**eriodically **R**otated **O**verlapping **P**arall**EL** **L**ines with **E**nhanced **R**econstruction) it acquires a number of parallel lines, each rotated about its centre through a series of angles in order to fully sample k-space (Figure 12.17). The k-space path then resembles an aircraft propeller, the 'blades' being the rotating block of parallel lines, each acquired during a single echo train. Radial TSE takes $\pi/2$ times longer than a conventional Cartesian TSE acquisition, e.g. in order to match a conventional acquisition with an N_{PE} of 480 lines, using a radial acquisition with an ETL of 28, would require $(480 \div 28) \times \pi/2 \approx 27$ blades. The scan time would therefore be TR × 27.

The advantage of using radial TSE is that the centre of k-space is heavily oversampled, reducing any artefacts due to patient motion. Furthermore, since each blade samples the centre of k-space any rotational or translational motion between blades during the reconstruction can be identified by any inconsistencies between each blade. Depending upon the similarity between blades, data can either be corrected to account for the motion or individual blades may even be discarded.

Radial TSE can produce good-quality images even in the presence of quite severe motion. Figure 12.18 shows two T_2-weighted TSE acquisitions in a normal volunteer who was asked to rotate their head from side to side during a conventional TSE acquisition

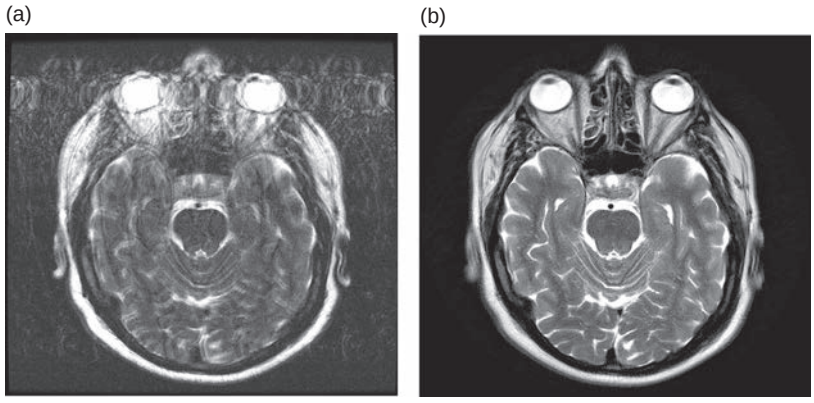

Figure 12.18 Effect of head motion on (**a**) conventional TSE (scan time 2 min 41 s) and (**b**) PROPELLER (scan time 3 min 12 s).

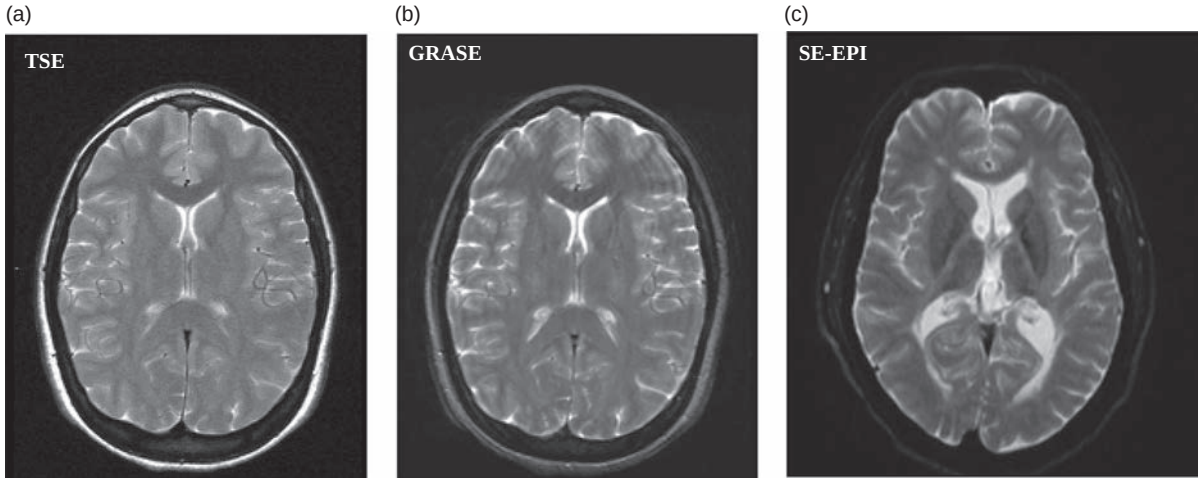

Figure 12.19 TSE, GRASE and SE-EPI images. (**a**) TSE, ETL = 5, TR = 2735 ms, TE = 102 ms, NSA = 2, scan time 3 min 32 s. (**b**) GRASE, turbo factor = 7, EPI factor = 3, TR = 3735 ms, TE = 132 ms, scan time 34 s. (**c**) SE-EPI, single shot, TE = 109 ms, scan time = 0.2 s per slice. Note the different appearance of the scalp fat between the sequences. The EPI uses fat suppression and exhibits significant distortion. Ringing artefacts are evident for GRASE

and a radial acquisition. It can also be used with diffusion weighting and, although significantly slower than EPI, the use of a TSE readout means that susceptibility issues are significantly reduced and that the overall image SNR is much higher. The issue of patient motion during the extended acquisition time is addressed by the inherent motion correction. Chapter 14 contains more detail about radial acquisitions.

12.5 Combining Gradient and Spin Echoes

A branch of the SE family tree involves sequences that utilize both spin and gradient echoes: GRASE and SE-EPI. As their contrast behaviour is more akin to conventional SE they are considered in this chapter. 2D GRASE is not often used, although 3D GRASE is recommended for readout in **A**rterial **S**pin **L**abelling (ASL – see Chapter 18). GRASE is a logical precursor to EPI, while SE-EPI is most commonly encountered in diffusion-weighted imaging (DWI) and diffusion tensor imaging (DTI). Representative images are shown in Figure 12.19.

12.5.1 GRASE

GRadient **A**nd **S**pin **E**cho (GRASE) or **T**urbo **G**radient **S**pin **E**cho (TGSE) is a fast segmented sequence that combines a multiple spin-echo train and intermediate gradient echoes, each with distinct values of phase encoding (Figure 12.20). Although it is a hybrid sequence, we class it in the spin-echo section as its

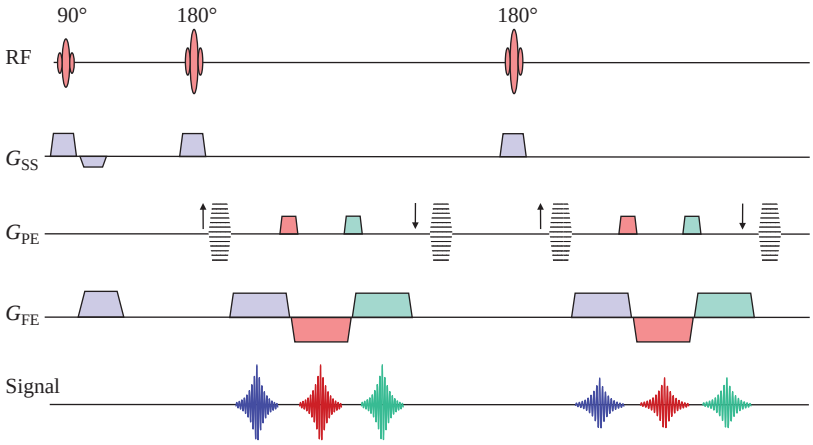

Figure 12.20 GRASE sequence diagram with three gradient and two spin echoes giving six lines of k-space per TR period.

behaviour and use are along the lines of spin echo. The scan time for GRASE is

$$\text{Scan time} = \frac{\text{TR} \times N_{\text{PE}}}{N_{\text{spin echoes}} \times N_{\text{gradient echoes}}}$$

Some systems call the number of spin echoes the 'turbo factor' and the number of gradient echoes the 'EPI factor'. Typically three gradient echoes will be used for each spin echo. The advantages of this are that much less RF power is used and that higher 'turbo factors' can be achieved. It is sometimes claimed that GRASE contrast is more like T_2-weighted spin echo than TSE (see Box 'Is TSE the Same as SE?'), although its current clinical use is not yet widespread. The complicated k-space scheme (see Box 'Grace Notes: k-Space Schemes for GRASE') can lead to substantial ringing artefacts in the phase-encode direction.

Grace Notes: k-Space Schemes for GRASE

Figure 12.21 shows the k-space scheme for the GRASE sequence of Figure 12.20 with a turbo factor of 2 and an EPI factor of 3. The 180° pulse is followed by a conventional phase-encode gradient, determined by a phase-encode table. However, fixed phase-encode gradients are used for the gradient-echo portion of the acquisition. These cause big fixed-length jumps in k-space, with phase changes being additive from the previous echoes for the current refocusing cycle. The phase encoding is rewound before the next RF and the phase-encode table will increment for the next spin echo. Thus successive lines of k-space will be subject to a T_2 decay envelope, with this pattern repeated periodically over k-space in the phase-encode axis. This results in the ringing or ghosting artefacts seen in the image in Figure 12.19b. As for TSE the contrast is dominated by the echo time used to acquire the centre of k-space.

12.5.2 Echo Planar Imaging

Spin-**E**cho-based **E**cho **P**lanar **I**maging (SE-EPI) can be regarded as an extreme case of GRASE, where a single excitation is given and the whole of k-space is sampled with gradient echoes under a single spin echo (Figure 12.22). It produces sequential slices in less than 100 ms with low spatial resolution, but is prone to artefacts. It is primarily used in dynamic or diffusion-weighted imaging. When using EPI, what immediately strikes you is that it sounds very different from other sequences, giving a single very loud, moderately high-pitched beep. Within this beep the whole of one slice is acquired, the sound being generated by a rapidly oscillating read gradient. EPI can be single or multi-shot, spin- or gradient-echo based. Here we consider the spin-echo version, SE-EPI. EPI contrast can be amazing. In single-shot EPI, TR is effectively infinite. Thus one can obtain very highly T_2- weighted contrast with no T_1 contribution at all.

In EPI the series of phase-encode gradients are replaced by small 'blips' placed at each readout gradient reversal. Each blip is of constant size and adds further phase encoding to the previous blips, resulting in a regular path through k-space (Figure 12.23), leading to a conventional 2D FT reconstruction. Large

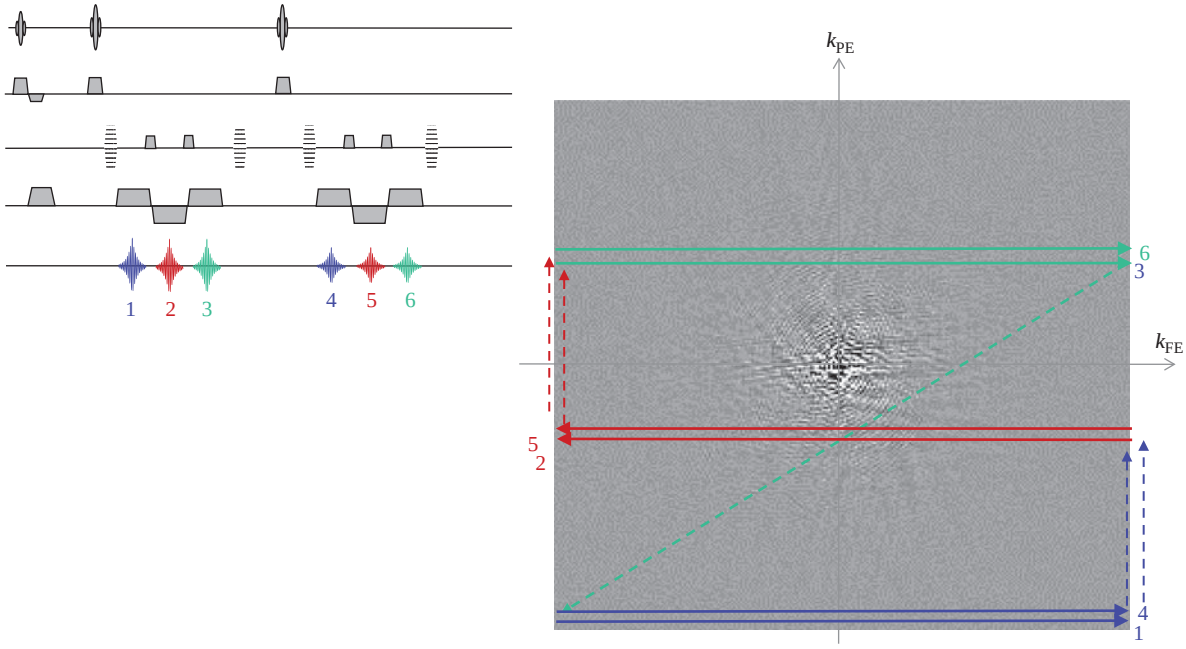

Figure 12.21 k-space acquisition for GRASE with two spin echoes and three gradient echoes. The k-space path corresponding to each echo is numbered.

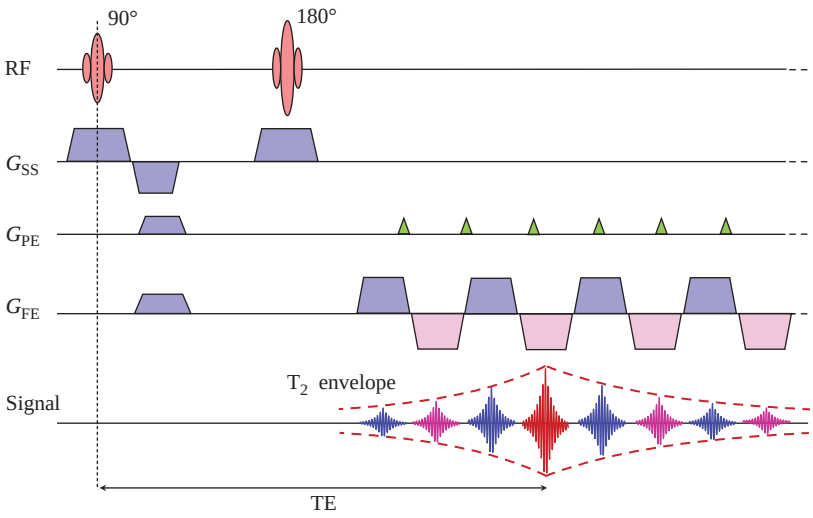

Figure 12.22 SE-EPI sequence diagram. Only eight echoes are shown. In practice 64 or 128 may be used.

read gradient amplitudes are required so that the appropriate values of k_{FE} can be sampled quickly, and the whole set of k_{PE} collected within a single spin echo envelope. This limits single-shot EPI acquisitions to the order of 100 ms, resulting in a typical resolution of 64 × 64 or 128 × 128. The time limitation imposed by the duration of the echo means that in EPI data are usually acquired during the gradient ramp-up times.

As for other segmented sequences, an effective echo time, where the centre of k-space is acquired, applies. Because the phase encoding is accrued monotonically, line-by-line, TE is generally of moderate length (e.g. 30–60 ms).

12.5.3 Image Quality in EPI

EPI is notorious for a high level of artefact. The classic EPI artefact is the *N*/2 (or 'Nyquist') ghost (Figure 12.24a), a phase ghost separated by exactly one-half the field of view. This arises because of imperfections in the rephasing–dephasing cycle of the rapidly switching bipolar frequency-encode gradient caused by eddy currents, resulting in alternate lines of k-space being misaligned (see Box 'Exorcism!'). In practice, a ghost level of a small percentage is almost always present.

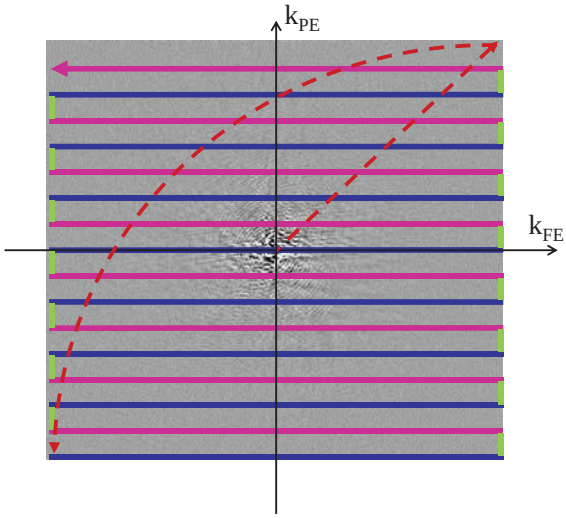

Figure 12.23 EPI k-space. The colours of the trajectory correspond to the similarly coloured gradient components in Figure 12.22.

The other artefacts are consequences of bandwidth. Each frequency-encode lobe is sampled rapidly with a very high gradient amplitude resulting in a very large signal bandwidth. The phase encode is sampled 64 or 128 times over the whole gradient-echo train. This rather slow sampling rate means that the signal bandwidth in the phase-encode direction may be as little as 10 Hz per pixel. This has two major consequences.

First, chemically shifted signals from fat will be displaced by many pixels, a significant fraction of the entire field of view in the phase-encode direction (Figure 12.24b). For this reason effective fat suppression is mandatory in EPI.

Second, small magnetic field differences (of the order of 1 ppm) will result in much greater spatial distortion. In particular, air–tissue boundaries will result in large image distortions. Additionally, signal drop-out may occur for locally shortened T_2^*. The orientation of tissue–air boundaries within the magnet can dramatically influence the extent and nature of these effects. Regions of brain close to the nasal sinuses, auditory meatus, frontal and temporal lobes are particularly affected (Figure 12.24c).

Exorcism!

The origin of the *N*/2 ghost is a slight mispositioning of every alternate refocusing of the FID, resulting from gradient imperfections (Figure 12.25), which result in a misregistration of alternate lines of k-space. Phase correction can be derived from a

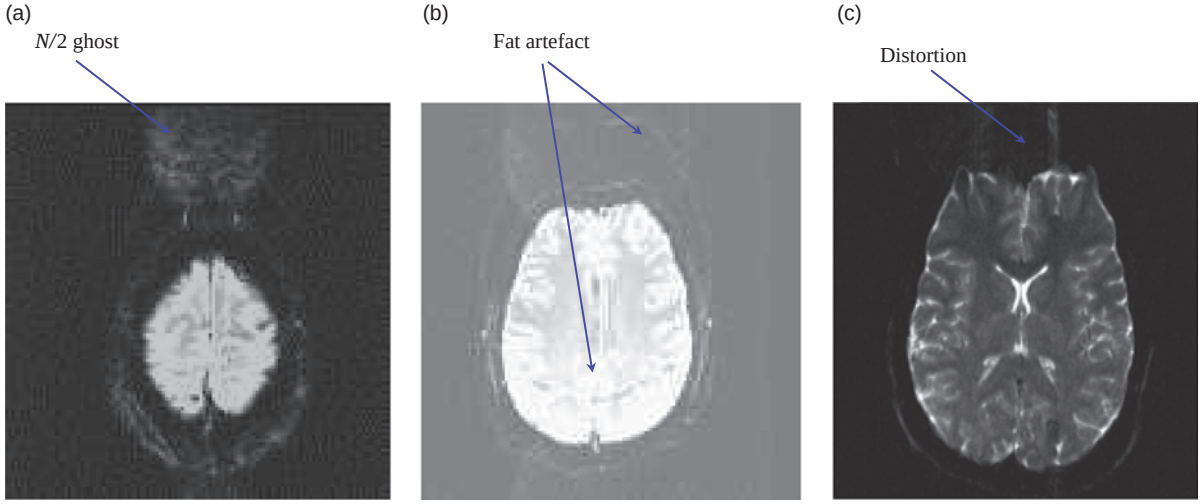

Figure 12.24 EPI artefacts: (a) *N*/2 (Nyquist) ghosts in the PE direction; (b) chemical shift – scalp fat is displaced by several pixels in the PE direction; (c) distortion in the frontal lobe.

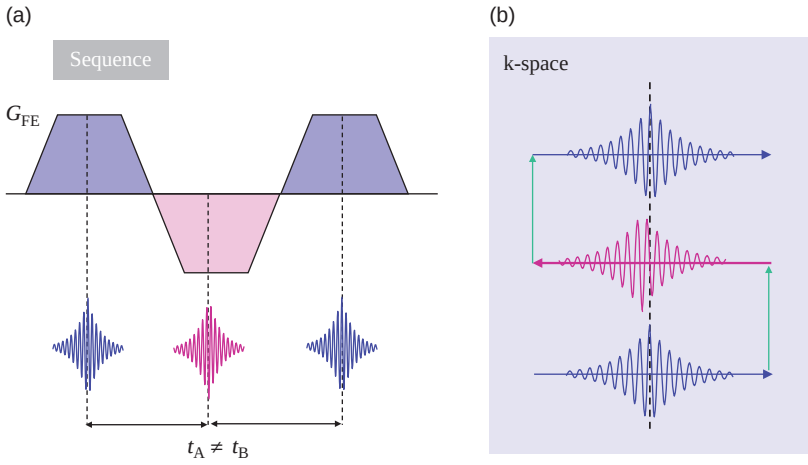

Figure 12.25 Origin of the Nyquist ghost in EPI. Timing errors result in misplacement of the centre of the consecutive echoes.

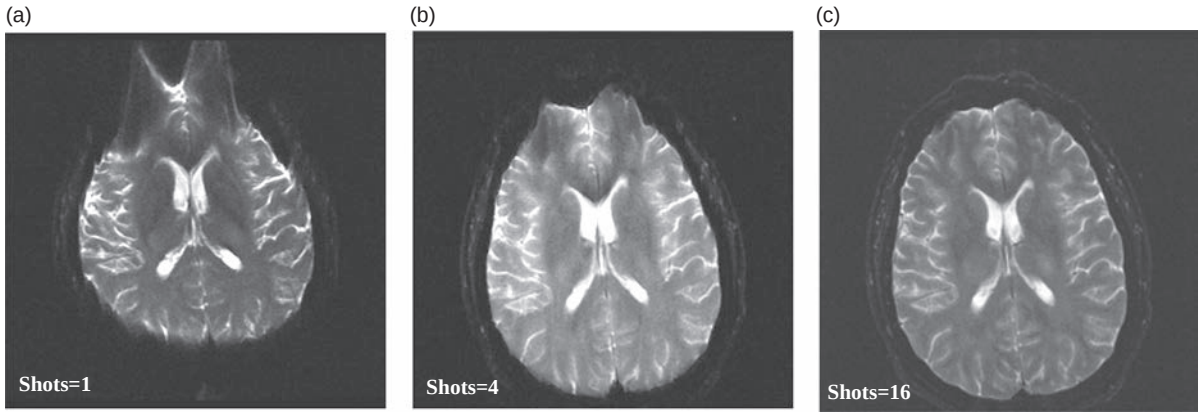

Figure 12.26 (a) Examples of extreme spatial distortion in single-shot EPI and improvements for multi-shot EPI; (b) 4 shots; (c) 16 shots.

reference scan which is identical to a full scan but without phase encoding. From the 1D FT of these data lines, phase correction filters can be produced which will then be applied to every line of image data. Phase correction is also used in RARE imaging techniques. Additionally, the position of the sampling points (the ADC raster) may be shifted to ensure the echoes are all centred. This requires a substantial pre-scan calibration procedure. To reduce artefacts, shimming using the gradients is required before an EPI acquisition. Even so, *N*/2 ghosts are almost always a small percentage of the main image signal.

12.5.4 Multi-Shot EPI

In multi-shot EPI, k-space is divided into two, four or eight segments, each of which is acquired by separate EPI trains. The advantages are that

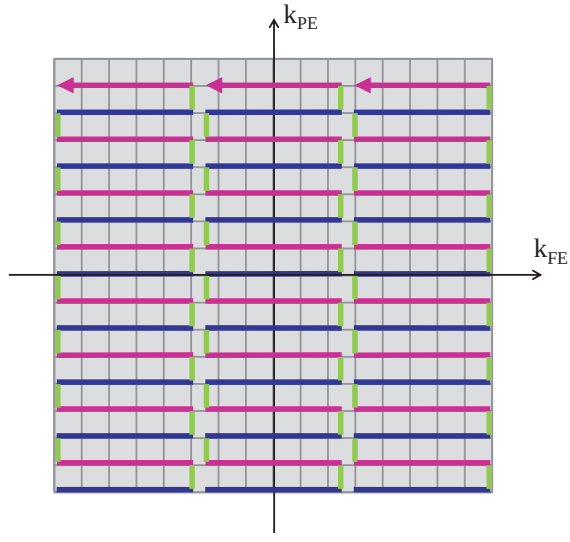

Figure 12.27 k-space trajectories for multi-shot EPI segmented in frequency encode. The entire k-space is covered in three shots.

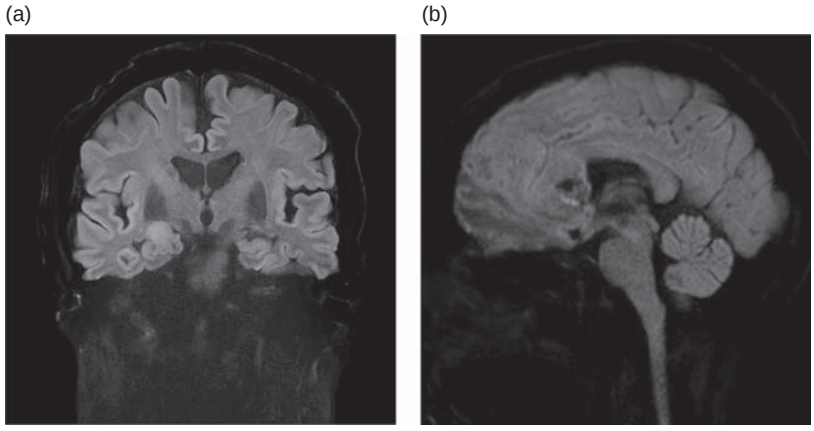

Figure 12.28 Multi-shot EPI using RESOLVE: (**a**) coronal, (**b**) sagittal. Note the lack of spatial distortion. Courtesy of Siemens Healthcare.

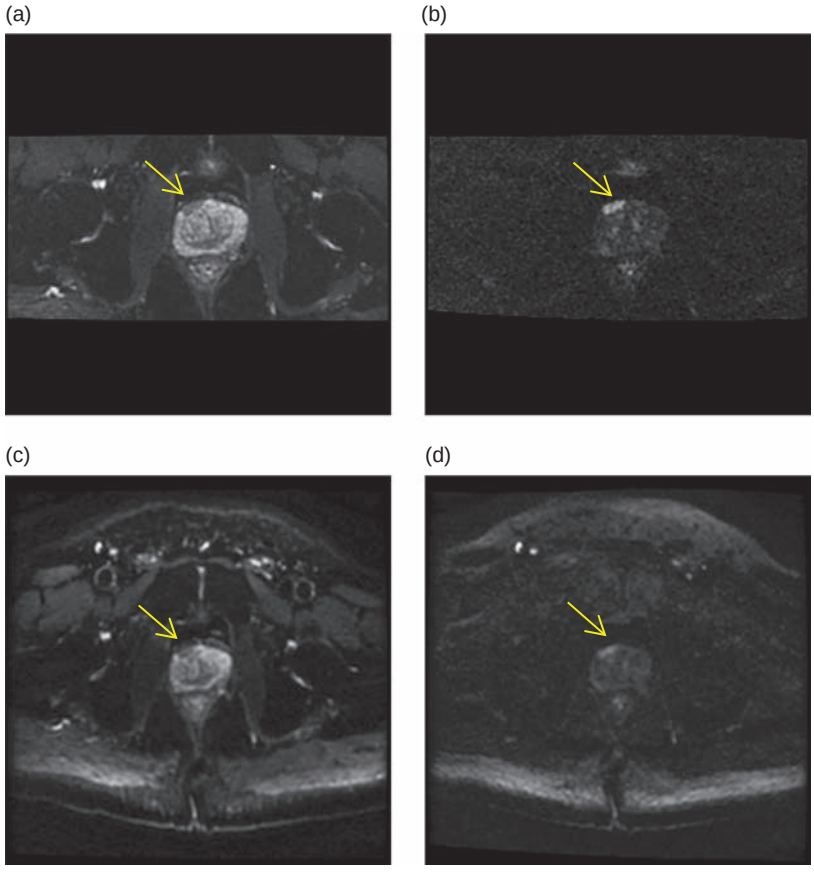

Figure 12.29 Standard DWI-EPI compared with reduced field-of-view (RFOV) DW-EPI using 2D RF excitation in the prostate. (**a**) and (**b**) RFOV DW-EPI with (**a**) b = 100 s mm^{-2} and (**b**) b = 1400 s mm^{-2}. Standard DW-EPI sequence with (**c**) b = 100 s mm^{-2} and (**d**) b = 1400 s mm^{-2}. Note the improved image quality with the RFOV acquisition.

susceptibility effects can be reduced as the PE bandwidth is effectively higher than for an equivalent single shot (Figure 12.26). Scan time is obviously increased and there is a need for a finite TR as in conventional scanning. Multiple-slice interleaving is possible, thereby helping to keep overall acquisition times short. The acquisition of 20 slices in 30 s, for example, is quite reasonable; however, the snapshot ability to freeze physiological motion is compromised.

A variation on multi-shot EPI is to acquire the segmentation in the frequency-encode direction

(Figure 12.27). This allows for better motion correction in addition to improving the level of distortion. This sequence is useful for body or spine diffusion imaging and is called RESOLVE on Siemens scanners. Another EPI development is to have multi-dimensional RF selective excitation. This can be used to produce small FOV EPI scans. FOCUS by GE Healthcare is one example. Images using RESOLVE and FOCUS are shown in Figure 12.28 and Figure 12.29 respectively.

See also:

- How frequency and phase-encoding gradients work: Chapter 7
- Basic image contrast: Chapter 3
- Introduction to pulse sequences: Chapter 4
- MRI Glossary

Further Reading

Bernstein MA, King KF and Zhou XJ (2004) *Handbook of MRI Pulse Sequences*. London: Elsevier Academic Press.

Brown MA and Semelka RC (1999) 'MR imaging abbreviations, definitions and descriptions: a review'. *Radiology* 213:647–662.

Brown RW, Cheng YCN, Haacke EM, Thompson MR and Venkatesan R (2014) *Magnetic Resonance Imaging: Physical Principles and Sequence Design*, 2nd edn. Hoboken, NJ: John Wiley & Sons, chapters 18 and 26.

Elster AD and Burdette JH (2001) *Questions and Answers in Magnetic Resonance Imaging*, 2nd edn. London: Mosby-Yearbook, chapters 5 and 12. Also on the web at http://mri-q.com [accessed 23 March 2015].

Haacke EM and Tkach JA (1990) 'Fast MR imaging: techniques and clinical applications'. *Am J Roentgen* 155:951–964.

Liney G (2011) *MRI from A to Z*, 2nd edn. London: Springer-Verlag.

Mansfield P and Maudsley AA (1977) 'Medical imaging by NMR'. *Br J Radiol* 50:188–194.

ReviseMRI.com (n.d.) 'MRI abbreviations'. www.revisemri.com/questions/misc/mri_abbrev [accessed 24 October 2013].

Twieg DB (1983) 'The k-trajectory formulation of the NMR imaging process with applications in analysis and synthesis of imaging methods'. *Med Phys* 10:610–623.